Theoretical Studies of Ag−Ag Closed-Shell Interaction in the Silver(I) Dimer Bis-μ-(5,7-dimethyl[1,2,4]triazolo[1,5-*a*]pyrimidine) Dinitrato Disilver(I): A RHF and Density Functional Study

Jaouad El-Bahraoui, Jose Molina Molina,* and Dolores Portal Olea

Grupo de Modelización y Diseño Molecular, Instituto de Biotecnología, Universidad de Granada, Granada 18071, Spain

Received: April 24, 1997; In Final Form: September 12, 1997

Calculations on $[Ag(NHCHNH)]_2$ and $[Ag(dmtp)(NO_3)]_2$ complexes have been performed at RHF, DFT (B3LYP), and MP2 levels. Geometry optimizations have been performed on both compounds comparing the result obtained with the different levels of theory and basis set against the available experimental X-ray data. The existence of M···M interaction at the different levels has been studied on both complexes using the Bader "Atoms in molecules" methodology.

Introduction

Metal−Metal interactions are still ambiguous in polynuclear silver(I) compounds. In disilver(I) complexes containing an eight-membered Ag−N−C−N−Ag−N−C−N ring, silver−silver distances between 2.655 and 3.187 Å have been found,[1−7] a few of these values being lower than twice the metallic silver radius (2.889 Å). Analogous rings are also known for Cu(I)[4,5,8] and Au(I).[6]

The possibility of silver−silver bonding in these compounds has been discussed in these references, concluding that the short distance between silver atoms does not necessarily mean that a bond is formed. Cotton et al.,[4] in a paper on molecular orbital calculations of the complex $Ag_2(form)_2$ (with form = *N*,*N*′-di-*p*-tolylformamidinato) using the SCF-Xα-SW method, conclude that no significant amount of net Ag−Ag bonding emerges. Furthermore similar calculations made on a Cu(I) dimer with a short copper−copper distance conclude that the interaction is repulsive.[4,9]

However, studies carried out by Perrault et al.[10] of the complex $Ag_2(dmpm)_2Br_2$ (dmpm = bis(dimethylphosphine)) and other related complexes with Ag−Ag distances in the range 3.04−3.60 Å, show that intense Raman scatterings appear associated with the metal−metal stretching. Likewise, it is important that there are metal complexes such as $[Ag(NH_3)_2]_2$-SO_4[11] or Ag(2-hydroxypyrimidinato)·$2H_2O$,[12] with silver atoms linearly coordinated and without supporting bridging ligands, in which distances Ag−Ag (3.200 and 3.302 Å, respectively) are shorter than twice the van der Waals radius (3.44 Å),[13] this interaction playing a substantial role in the crystal packing.

Very recently studies on closed-shell interactions between heavy metals have been reported on Au(I) complexes,[14−18] in which the importance of including the relativistic effect in the calculation is pointed out. Also a general review on such interaction is available.[19]

A study of d^{10}−d^{10} closed-shell interaction in rings, including eight-member rings, and metals such as Au^I, Ag^I, and Cu^I will also be available.[20]

Our group is involved in a project that studies binuclear complexes of transition metals with biological interest; on this subject we have presented results in model[21] and triazolopyrimidine binuclear complexes.[22,23]

In a recent study of $[Ag(dmtp)(NO_3)]_2$, where dmtp represents the ligand 5,7-dimethyl[1,2,4]triazolo[1,5-*a*]pyrimidine,[22] we presented a structural and RHF single-point calculation study in which we reached the conclusion that a direct interaction between the two metal centers has been found, on the basis of the properties of the charge density distribution derived from ab initio MO calculation of experimental geometry. Similar conclusions have been obtained for the model compound $[Ag(NHCHNH)]_2$ after performing a geometry optimization at the RHF level. This work is a continuation of that paper in which we performed a comparison between RHF, MP2, and density functional studies using both all-electron and ECPs basis sets on the model compound $[Ag(NHCHNH)]_2$, for which no metal−metal interactions have been proposed by Cotton.[4] This comparison has been limited to RHF and DFT in the complex $[Ag(dmtp)(NO_3)]_2$ in order to study the theoretical description of these compounds including the possible Ag−Ag interaction.

Computational Methods

Ab initio MO calculations for the model compound $[Ag(NHCHNH)]_2$ have been performed through the GAUSSIAN-94 series of programs[24] using restricted Hartree−Fock (RHF), MP2(full), and density functional theory[25] on a SGI Power Challenger machine. Among the characteristics of this code for DFT methodology are the use of Gaussian basis functions, the avoidance of auxiliary functions, the implementation of large grids, and the availability of analytical first and second derivatives.[26,27]

In hybrid methods the exchange−correlation energy (E_{XC}) is represented by the following general equation:

$$E_{XC} = a_0E_X^{UEG} + (1 - a_0)E_X^{HF} + a_X\Delta E_X + E_C^{UEG} + a_C\Delta E_C \quad (1)$$

where E_X^{UEG} is the density functional for the exchange energy of the uniform electron gas,[28] E_C^{UEG} is the corresponding correlation contribution,[29] E_X^{HF} is the Hartree−Fock exchange, and the ΔE terms are the gradient correction contributions to exchange and correlation.

* Author for correspondence. jmolina@goliat.ugr.es.

S1089-5639(97)01389-3 CCC: $15.00
Published on Web 03/13/1998

TABLE 1: Selected Bond Distances (Å) and Bond Angles (deg) for $[Ag(NHCHNH)]_2$ at Different Levels of Theory

level of theory	Ag−Ag	Ag−N	C−N	N−Ag−N	N−C−N
HF/STO-3G*	2.549	2.082	1.333	174.5	123.54
MP2(Full)/STO-3G*	2.525	2.041	1.363	176.29	122.81
B3LYP/STO-3G*	2.449	2.035	1.362	176.82	122.34
HF/Basis2	2.897	2.244	1.305	165.36	125.87
MP2(Full)/Basis2	2.793	2.190	1.325	168.44	125.18
B3LYP/Basis2	2.762	2.159	1.322	169.02	125.35
HF/LANL2DZ	2.978	2.184	1.323	163.64	125.88
MP2(Full)/LANL2DZ	2.885	2.145	1.356	167.14	124.86
B3LYP/LANL2DZ	2.857	2.108	1.339	167.06	125.58
ref 20 1f HF	2.832	2.169	1.273	164.8	124.8
ref 20 1f MP2	2.726	2.082	1.306	168.7	124.8
ref 20 2f HF	2.867	2.171	1.303	165.7	126.3
ref 20 2f MP2	2.712	2.043	1.322	169.9	125.4
experiment[4]	2.705	2.105	1.299	168.8	124.9

A hybrid method is further qualified as self-consistent when gradient correction and RHF exchange are not simply computed using a converged LSD wave function (or, more traditionally, LSD and gradient correct contributions added to a converged RHF wave function), but the SCF process is performed with the complete density functional. The B3LYP variant is obtained using the Becke gradient correction to exchange[30] and the Lee−Yang−Parr (LYP) correlation functional.[31] Since the LYP functional contains both a local part and a gradient correction, only the latter contribution should be used to obtain a coherent implementation. It is, however, expedient to use the approximation

$$\Delta E_C \approx E_C^{LYP} - E_C^{VWN} \quad (2)$$

A number of tests showed that values of the three semiempirical coefficients, appearing in eq 1, near 0.80 provide the best results, irrespective of the particular form of the different functionals. The values ($a_0 = 0.80$, $a_X = 0.72$, $a_C = 0.81$) determined by Becke from a best fitting of the heats of formation of a standard set of molecules[32] have been used.

D_{2h} symmetry restricted geometry optimizations were carried out for $[Ag(NHCHNH)]_2$, and geometry optimizations were performed taking the complete structure of $[Ag(dmtp)(NO_3)]_2$ with the original C_i symmetry. STO-3G*,[33] LANL2DZ,[34] and Basis2 (means 3-21G[35] on Ag and 6-31G* for C, N, H) basis sets have been used through the calculation. The LANL2DZ basis set uses D95[36] on the first row and Hay and Wadt's large-core quasirelavistic effective core potential (LANL2)[37] basis set on the Ag atom.

Result and Discussion

1. Calculation on $[Ag(NHCHNH)]_2$. Studies of Ag−Ag interaction have been performed on $[Ag(NHCHNH)]_2$ by Cotton et al., using the SCF-Xα-SW method;[4] from an analysis of the corresponding molecular orbitals, they concluded that no significant amount of net Ag−Ag bonding emerges. In a previous research on that complex[22] we proposed that a significant metal−metal interaction emerges from the topological analysis of the charge density studied from the RHF/STO-3G* and LANL2DZ wave functions. In this work a comparison of calculations at the RHF, MP2, and DFT levels with STO-3G*, Basis2, and LANL2DZ is presented. Full geometry optimization of $[Ag(NHCHNH)]_2$ keeping D_{2h} symmetry is performed at the different levels. The results are shown in Table 1, including the selected optimized geometrical parameters of $[Ag(NHCHNH)]_2$ at different levels of the theory. Experimental values for a very related complex $[Ag_2(form)_2]$, where (form) represents the anion of [(*p*-tol)NCHNH(*p*-tol)],[4] are also shown for comparison together with theoretical values form Pyykkö et al.[20] at RHF and MP2 levels using the Stuttgart pseudopotential and one or two f polarization functions on Ag atoms. From Table 1 the following conclusions can been extracted.

The STO-3G* basis set is not accurate at the different levels performed, giving geometries with Ag−Ag and Ag−N distances very short and the corresponding C−N too large in comparison with the experimental ones. The use of a split valence basis set Basis2 or a full double-zeta LANL2DZ improves notably the geometry at the RHF level, but giving Ag−Ag distance still too large.

These two last basis sets Basis2 and LANL2DZ with hybrid functional B3LYP give comparable geometrical parameters. However the best results are shown at the B3LYP/LANL2DZ level, which are very close to the experiment. From the above consideration we can point out the importance of using the ECPs basis set corrected for relativistic effects together with hybrid density functional theory in the theoretical study of transition metal complexes. However, the use of Basis2 together with a hybrid functional gives also very good results (see Table 1). To test the validity of the results obtained from DFT, MP2 (full) calculations with the different basis sets used have been performed and also comparisons have been done with theoretical (RHF and MP2) from Pyykkö et al.[20] (see Table 1).

The results obtained from MP2 are in general agreement with the B3LYP with the basis sets used and with the experimental results. The agreement between our theoretical results is very good for N−Ag−N and N−C−N angles and Ag−N distance. The main difference came from the Ag−Ag distance. Our data are also in agreement with the RHF and MP2 results from ref 20.

In general it is necessary to point out the importance of the good theoretical description of the ligand and the usefulness to include polarization functions.

Taking into account that the STO-3G* calculations show a very poor geometry, the following discussion about the metal−metal interaction is performed with the Basis2 and LANL2DZ basis sets at the RHF, DFT, and MP2 levels.

The topology of the electronic charge density, $\rho(r)$, as pointed out by Bader,[38] is a faithful mapping of the chemical concepts of atoms, bonds, and structure. The principal topological properties are summarized in terms of its critical points (CPs).[38,39] The nuclear positions behave topologically as local maxima in $\rho(r)$. A bond critical point (BCP) is found between every pair of nuclei, linked by a chemical bond, with two curvatures negative and one positive. The ring critical points (RCPs) are characterized by a single negative curvature.

Each (3,−1) CP generates a pair of gradient paths[38] which originate at CP and terminate at neighboring attractors; this gradient path defines a line through the charge distribution linking the neighboring nuclei along which $\rho(r)$ is a maximum with respect to any neighboring line. Such a line is referred to as an atomic interaction line.[38,39]

The presence of an atomic interaction line in such an equilibrium geometry satisfies both the necessary and sufficient condition that the atoms be bonded together. The Laplacian of $\rho(r)$, $\nabla^2\rho(r)$, determines two extreme situations, where ρ is locally concentrated ($\nabla^2\rho(r) < 0$) at a BCP unambiguously related to a covalent bond, showing that a sharing of charge has taken place. However, in a closed-shell interaction a value of $\nabla^2\rho(r) > 0$ is expected, such as found in noble gas repulsive states, in ionic bonds, in hydrogen bonds, etc.

TABLE 2: Charge Density ρ_r (e/a_0^3), Laplacian of the Charge Density $\nabla^2\rho_r$ (e/a_0^5), Curvatures (λ_1, λ_2, λ_3) (e/a_0^5), Ellipticities ϵ, and Local Energy Density $E_d(r)$

level of theory	ρ_r	$\nabla^2\rho_r$	λ_1	λ_2	λ_3	ϵ	$E_d(r)$
			Ag−Ag (CP)				
HF/Basis2	0.021	0.069	−0.020	−0.019	0.108	0.035	−0.004
MP2(Full)/Basis2	0.041	0.101	−0.035	−0.033	0.170	0.061	−0.006
B3LYP/Basis2	0.033	0.080	−0.028	−0.027	0.136	0.061	−0.009
HF/LANL2DZ	0.018	0.747	−0.013	−0.013	0.102	0.0136	−0.001
MP2(Full)/LANL2DZ	0.036	0.124	−0.028	−0.027	0.180	0.049	−0.002
B3LYP/LANL2DZ	0.027	0.095	−0.021	−0.019	0.136	0.062	−0.001
			Ag−N (CP)				
HF/Basis2	0.064	0.326	−0.072	−0.067	0.466	0.084	−0.003
MP2(Full)/Basis2	0.092	0.473	−0.114	−0.107	0.694	0.064	−0.006
B3LYP/Basis2	0.077	0.392	−0.090	−0.084	0.567	0.073	−0.004
HF/LANL2DZ	0.077	0.336	−0.090	−0.084	0.509	0.076	−0.018
MP2(Full)/LANL2DZ	0.105	0.435	−0.130	−0.122	0.689	0.063	−0.021
B3LYP/LANL2DZ	0.090	0.377	−0.108	−0.101	0.587	0.070	−0.023
			Ag−N−Ag (CP)				
HF/Basis2	0.008	0.036	−0.005	0.013	0.028		
MP2(Full)/Basis2	0.015	0.057	−0.009	0.026	0.040		
B3LYP/Basis2	0.011	0.044	−0.007	0.018	0.032		
HF/LANL2DZ	0.009	0.032	−0.005	0.012	0.025		
MP2(Full)/LANL2DZ	0.015	0.058	−0.008	0.026	0.040		
B3LYP/LANL2DZ	0.012	0.044	−0.006	0.019	0.032		

Furthermore, Bader defined a local electronic energy density, $E_d(r)$, as a functional of the first-order density matrix

$$E_d(r) = G(r) + V(r) \tag{3}$$

where $G(r)$ and $V(r)$ correspond to a local kinetic and potential energy density, respectively.[38] The sign of $E_d(r)$ determines whether accumulation of charge at a given point r is stabilizing ($E_d(r) < 0$) or destabilizing ($E_d(r) > 0$). Thus, a value of $E_d(r) < 0$ at a BCP shows a significant covalent contribution and, therefore, a lowering of the potential energy associated with the concentration of charge between the nuclei. Also, very recently, Grimme[40] has found for some saturated and unsaturated hydrocarbons a linear correlation between the bond energies, the local electronic energy density $E_d(r)$ and $\rho(r)$ at the position of the BCP.

Calculations of the CP on the charge density have been performed by the Extreme program[41] from the corresponding wave function.

The numerical results have been summarized in Table 2, in which the charge density ρ, the Laplacian of the charge density $\nabla^2\rho(r)$, the corresponding curvatures, and the ellipticity ϵ for the BCPs at different levels are shown. Figure 1 shows the contour map of the electron charge density, $\rho(r)$ (a), and its Laplacian (b) for the $[Ag(NHCHNH)]_2$ eight-membered plane. As shown in Figure 1, the charge density shows local maxima only at the position of the nuclei. (3,−1) BCPs exist between the two Ag atoms and between the Ag and each of its nitrogen-bonded atoms, and BCPs can be found between C−N, C−H, and N−H atoms. Two RCPs are also found on the plane marked as stars in the figure. The contour representations of $\rho(r)$ for the different levels are completely equivalent, and only the representation for B3LYP/Basis2 is shown. Figure 1b shows the contour of the Laplacian of the charge density in the same plane; the thin lines denote positive Laplacian values, and the thick ones denote negative Laplacian values. As can be seen in Figure 1b, a region of negative Laplacian values can be located through the ligand denoting a covalent region (shared interaction). The region between the two Ag atoms and that between the Ag and all of its nitrogen-bonded atoms are of positive Laplacian regions showing closed-shell interactions. As shown in Table 2 for the different levels of calculation, a BCP between the two Ag atoms can be found, giving a value of the density charge between 0.02 and 0.04 e/a_0^3; the corresponding values for the Ag−N BCPs are between 0.06 and 0.1 e/a_0^3, showing that the $\rho(r)$ of the Ag−Ag CP is larger than one-third of the value between the metal−nitrogen BCP for the different levels of calculation. Both types of BCPs show values of $\nabla^2\rho(r)$ positive, but the value of the Ag−Ag CP is very small in comparison with the Ag−N values. The ellipticity for the

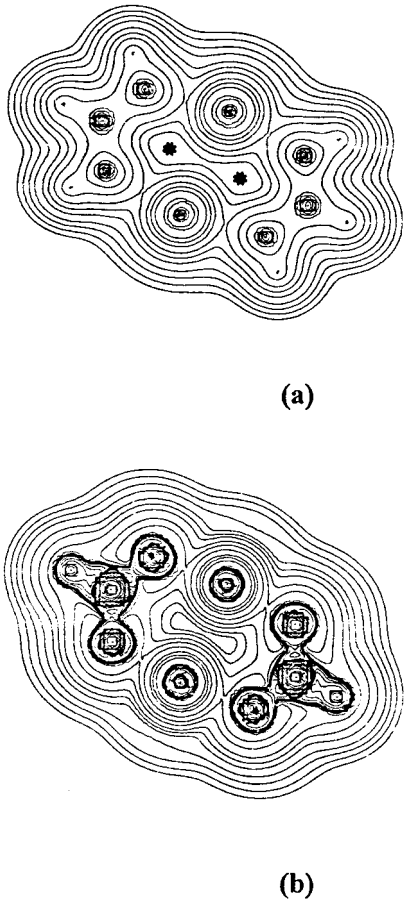

Figure 1. Contour plot of the (a) charge density (ρ) and (b) Laplacian of the charge density ($\nabla^2\rho_r$) for compound $C_2H_6Ag_2N_4$ at B3LYP/Basis2.

TABLE 3: Selected Bond Distances (Å) and Bond Angles (deg) for $[Ag(dmtp)(NO_3)]_2$ at Different Levels of Theory

distance	expt[16]	3-21G	LANL2DZ	angle	expt[16]	3-21G	LANL2DZ
				RHF			
Ag−Ag	3.058	3.025	3.118	N3−Ag−N4	162.3	167.901	164.142
Ag−N3	2.210	2.404	2.404	N3−Ag−O1	90.4	98.596	87.359
Ag−N4	2.250	2.839	2.578	N3−Ag−O2	108.7	115.874	102.896
Ag−O1	2.749	2.582	2.762	N4−Ag−O1	87.5	77.432	81.174
Ag−O2	2.816	2.469	2.553	N4−Ag−O2	81.7	70.935	77.649
N−O1	1.234	1.317	1.288	O1−Ag−O2	44.3	52.384	48.789
N−O2	1.225	1.301	1.287	O1−N−O2	117.3	116.971	117.642
N−O3	1.198	1.230	1.237				
				B3LYP			
Ag−Ag		2.886		N3−Ag−N4		164.1	
Ag−N3		2.303		N3−Ag−O1		87.4	
Ag−N4		2.602		N3−Ag−O2		102.9	
Ag−O1		2.552		N4−Ag−O1		81.1	
Ag−O2		2.762		N4−Ag−O2		77.6	
N−O1		1.287		O1−Ag−O2		48.8	
N−O2		1.288		O1−N−O2		117.6	
N−O3		1.238					

Ag−Ag CPs is also very small, showing a radial symmetry distribution of the $\rho(r)$ along the Ag−Ag axes. However the ϵ of the Ag−N CP is larger, showing some π bonding character.

Two symmetrically equivalent RCPs have been found for the two Ag−N−C−N−Ag rings, showing very small $\rho(r)$ and $\nabla^2\rho(r)$ on those points (see Table 2). The existence of the different mentioned CPs and, more specifically, the BCP and zero flux surface in the gradient vector of the charge density, which separates the basis of the two Ag atoms, is indicative of metal−metal bonding, taking into account that all topological analyses have been performed on a minimum of the potential energy surface.

From the above-mentioned topological analysis, it is clear that a metal−metal interaction should exist between the two Ag atoms, and studying the local energy density $E_d(r)$ at the BCP can show whether the accumulation of the charge at this point is stabilizing ($E_d(r) < 0$) or destabilizing ($E_d(r) > 0$); Table 2 shows the local energy density for different BCPs at different levels of calculation.

The values of the local energy density $E_d(r)$ at the Ag−Ag bond is negative and comparable to those of Ag−N bonds (see Table 2). However, the values expected for C−N BCPs are negative and large in comparison with the Ag−Ag and Ag−N BCPs, showing the covalent nature of the bond. The negative values of the energy density for the Ag−Ag and Ag−N BCPs show the stabilizing nature of the interaction and the small covalent character of these bonds.

2. Calculation on $[Ag(dmtp)(NO_3)]_2$. Theoretical studies on $[Ag(dmtp)(NO_3)]_2$ have also been performed with a special focus on Ag−Ag interaction. For this complex experimental crystallographic geometry is available from a previous paper,[22] in which a single-point calculation on the experimental geometry was performed. In the current work, full geometry optimization of the complex is presented starting from the experimental geometry and keeping the C_i symmetry, at the RHF/3-21G, RHF/LANL2DZ, and B3LYP/3-21G levels of theory; we are not able to use larger levels of theory due to the size of the system.

In Figure 2 the Pluto structure of the optimized complex at the B3LYP/3-21G is shown. The numerical results are presented in Table 3, in which the main geometry parameters are shown in comparison with the experimental ones.

From Table 3 we can point out that both basis sets give good structures. The Ag−Ag distances are well predicted; however, the 3-21G structure gives significant deviation for the same parameters. For example, the Ag−N_4 distance is predicted too large and the Ag−O_1 and Ag−O_2 ones too short. There are also substantial deviations in the description of the bond angles.

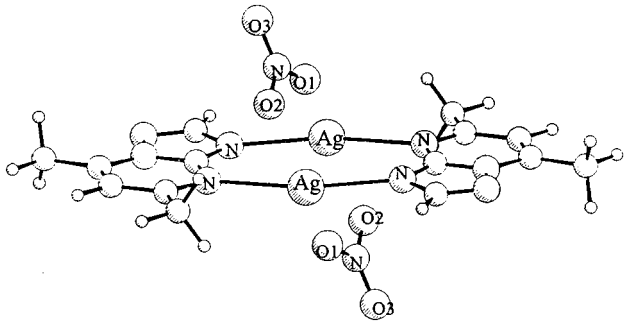

Figure 2. Theoretical Pluto presentation obtained for compounds $[Ag(dmtp)(NO_3)]_2$ at the B3LYP/3-21G level.

The LANL2DZ basis set corrects the above deficiency in the geometry description to a large degree, giving a geometry very close to the experiment. Nevertheless a small deviation still remains in the description of the Ag−Ag, Ag−N_3, and Ag−N_4 distances. DFT calculation on $[Ag(dmtp)(NO_3)]_2$ has been performed at the B3LYP/3-21G level. Attempts to do optimization at the B3LYP/LANL2DZ have always given different grid problems. However the result obtained at the B3LYP/3-21G level is the one that gives the better average geometry compared with X-ray data. All the above results show the importance of including electron correlation and relativistic effects in the study of the heavy metal complexes.

The experimental Ag−Ag distance for the $[Ag(dmtp)(NO_3)]_2$ complex is 3.058 Å, smaller than twice the van der Waals radius (3.44 Å), so metal−metal interaction should play an important role in the geometry description of the complex. We are going to study the Ag−Ag interaction using the topological analysis of the charge density following the Bader methodology. Table 4 shows numerical results for selected CPs of $[Ag(dmtp)(NO_3)]_2$ at the different levels studied, in which the values of ρ, $\nabla^2\rho(r)$, curvatures, and ϵ for the different CPs are presented. Figure 3 shows the contour of $\rho(r)$ in the eight-membered ring molecular plane (a) and the contour of $\nabla^2\rho(r)$ (b). From Figure 3a, BCPs can be found between both Ag atoms; also BCPs between the Ag and N atoms are found. Two RCPs are located in the eight-membered ring (Ag−N−C−N−Ag−N−C−N). From Figure 3b, negative values of the $\nabla^2\rho(r)$ can be located on the network of the ligand, showing the covalent character of the different bonds. The space surrounding the Ag−Ag and Ag−N BCPs

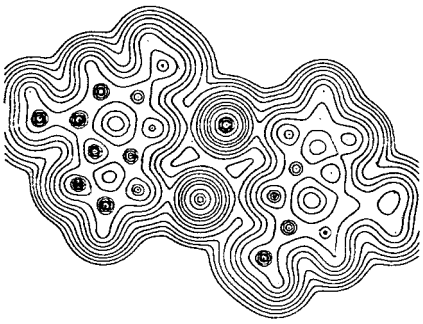

(a)

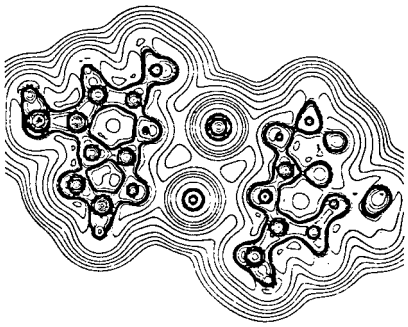

(b)

Figure 3. Contour plot of the (a) charge density (ρ) and (b) Laplacian of the charge density ($\nabla^2\rho_r$) for compound $[Ag(dmtp)(NO_3)]_2$ at B3LYP/3-21G.

TABLE 4: Charge Density ρ_r (e/a_0^3), Laplacian of the Charge Density $\nabla^2\rho_r$ (e/a_0^5), Curvatures (λ_1, λ_2, λ_3) (e/a_0^5), Ellipticities ϵ, and Local Energy Density $E_d(r)$

	ρ_r	$\nabla^2\rho_r$	λ_1	λ_2	λ_3	ϵ	$E_d(r)$
			RHF/3-21G				
Ag−Ag	0.013	0.056	−0.013	−0.009	0.079	0.322	−0.003
Ag···N3	0.046	0.198	−0.046	−0.044	0.290	0.044	−0.003
C···N3	0.336	−0.861	−0.745	−0.657	0.541	0.133	−0.66
Ag−O1	0.029	0.125	−0.030	−0.029	0.185	0.029	
Ag−O2	0.037	0.162	−0.040	−0.039	0.242	0.028	
ring	0.005	0.030	−0.003	0.009	0.024		
			RHF/LANL2DZ				
Ag−Ag	0.011	0.050	−0.008	−0.007	0.065	0.240	−0.001
Ag···N3	0.045	0.228	−0.050	−0.048	0.326	0.054	−0.021
C···N3	0.334	−0.858	−0.713	−0.623	0.478	0.145	−0.396
Ag−O1	0.018	0.091	−0.016	−0.015	0.124	0.072	
Ag−O2	0.028	0.156	−0.031	−0.029	0.216	0.074	
ring	0.004	0.016	−0.002	0.006	0.011		
			B3LYP/3-21G				
Ag−Ag	0.011	0.050	−0.008	−0.007	0.065	0.240	−0.001
Ag···N3	0.045	0.228	−0.050	−0.048	0.326	0.054	−0.002
C···N3	0.334	−0.858	−0.713	−0.623	0.478	0.145	−0.354
Ag−O1	0.018	0.091	−0.016	−0.015	0.124	0.072	
Ag−O2	0.028	0.156	−0.031	−0.029	0.216	0.074	
ring	0.004	0.016	−0.002	0.006	0.011		

shows a small but positive $\nabla^2\rho(r)$, indicating closed-shell interaction. The numerical values of $\rho(r)$ in the Ag−Ag BCP is between one-third and one-fourth the value of the Ag−N BCP (see Table 4) as found for the model compound. The value of $\nabla^2\rho(r)$ for Ag−Ag BCP is positive but very small (0.05 e/a_0^5); however, the values for Ag−N BCPs are around 0.2 e/a_0^5, showing an important ionic character in the Ag−N bonds.

The values of the local energy density $E_d(r)$ at the Ag−Ag bond are negative and comparable to those of Ag−N bonds (see Table 4). However, the values of the C−N BCP are negative and large in comparison with the Ag−Ag and Ag−N BCPs, showing the covalent nature of the bond. The negative values of the energy density for the Ag−Ag and Ag−N BCPs show the stabilizing nature of the interaction and small covalent character of these bonds.

Conclusion

From the calculation presented in this paper, we can conclude that the use of the hybrid RHF, DFT methodology could be suitable for geometry optimization on the study of binuclear transition metal complexes using at least a split valence basis set or a quasirelativistic corrected pseudopotential basis set. These results are also in general agreement with the MP2 calculations. This shows the importance of taking into account the correlation and relativistic effect in the theoretical description of these systems. It is also necessary to point out the importance of including polarization functions in the description of the ligands.

Acknowledgment. The authors thank **DGICYT** for financial support (Grant No. PB94-0807-CO2-02). We are grateful to Professor R. W. F. Bader for a copy of the **AIMPAC** package and Professor P. Pyykkö for sending us the preprint of ref **19** and **20**. We also thank Jill Dennis Lammert for correction of the original English manuscript.

References and Notes

(1) Smith, D. L.; Luss, H. R. *Photogr. Sci. Eng.* **1976**, 20.
(2) Baenziger, N. C.; Stuss, A. W. *Inorg. Chem.* **1976**, 15.
(3) Gagnon, C.; Huber, J.; Rivest, R.; Beauchamp, A. L. *Inorg. Chem.* **1977**, *16*, 2469.
(4) Cotton, F. A.; Feng, X.; Matusz, M.; Poli, R. *J. Am. Chem. Soc.* **1988**, *110*, 7077.
(5) Munakata, M.; Maekawa, M.; Kitayama, S.; Adachi M.; Masuda, H. *Inorg. Chim. Acta* **1990**, *167*, 181.
(6) Fenske, D.; Baum, G.; Zinn A.; Dehnicke, K. *Z. Naturforsch., Teil B* **1990**, *45*, 1273.
(7) Olbrich, F.; Zimmer, B.; Kastner, M.; von Schlabrendorff, C.; Vetter, G.; Klar, G. *Z. Naturforsch. Teil B* **1992**, *45*, 1571.
(8) Kitagawa, S.; Matsuyana, M.; Munakata, M.; Osawa, N.; Masuda, H. *J. Chem. Soc., Dalton Trans.* **1991**, 1717.
(9) Lee, S. W.; Trogler, W. C. *Inorg. Chem.* **1990**, *29*, 1659.
(10) Perreault, D.; Drouin, M.; Machel, A.; Miskowski, V. M. Schaefer, W.; Harvey, P. D. *Inorg. Chem.* **1992**, *31*, 695.
(11) Zachwieja, U.; Jacobs, H. *Z. Kristallogr.* **1992**, *201*, 207.
(12) Quirós, M. *Acta Crystallogr., Sect. C* **1994**, *50*, 1236.
(13) Bondi, A. *J. Phys. Chem.* **1964**, *68*, 441.
(14) Runeberg, N. *Relativistic Quamtum Chemical Stdies of New Heavy-Element Compounds.* Doctoral Thesis, University of Helsinki, Finland, 1996.
(15) Pyykkö, P.; Runeberg, N. *Chem. Commun.* **1993**, 1812.
(16) Pyykkö, P.; Li, J.; Runeberg, N. *Chem. Phys. Lett.* **1994**, *218*, 133.
(17) Pyykkö, P.; Zhao, Y. F. *Angew. Chem., Int. Ed. Engl.* **1991**, *30*, 604.
(18) Li, J.; Pyykkö, P. *Chem. Phys. Lett.* **1992**, *197*, 586.
(19) Pyykkö, P. *Chem. Rev.* **1997**, *97*, 597.
(20) Pyykkö, P.; Medizabal, F. *Chem. Eur. J.*, accepted.
(21) El-Bahraoui, J.; Molina, J.; Portal, D. *J. Mol. Structure*, accepted.
(22) Romero, M. A.; Salas, J. M.; Quirós, M.; Sánchez, M. P.; Molina, J.; El-Bahraoui, J.; Faure, R. *J. Mol. Struct.* **1995**, *354*, 189.
(23) Romero, M. A.; Salas, J. M.; Quirós, M.; Sánchez, M. P.; Molina, J.; El-Bahraoui, J. *Inorg. Chem.* **1996**, *35*, 7829.
(24) Frisch, M. J.; Trucks, G. W.; Schlegel, H. B.; Gill, P. M. W.; Johnson, B. G.; Robb, M. A.; Cheeseman, J. R.; Keith, T. A.; Petersson, G. A.; Montgomery, J. A.; Raghavachari, K.; Al-Laham, M. A.; Zakrzewski, V. G.; Otriz, J. V.; Foresman, J. B.; Cioslowski, J.; Stefanov, B. B.; Nanayakkara, A.; Challacombe, M.; Peng, C. Y.; Ayala, P. Y.; Chen, W.; Wong, M. W.; Andres, J. L.; Replogle, E. S; Gomperts, R.; Martin, R. L.; Fox, D. J.; Binkley, J. S.; Defrees, D. J.; Baker, J.; Stewart, J. P.; Head-Gordon, M.; Gonzales, C.; Pople, J. A. *Gaussian 94* (Revision C.2); Gaussian, Inc.: Pittsburgh, PA, 1995.

(25) (a) Parr, R. G.; Yang, W. Density-Functional Theory of Atoms and Molecules; Oxford University Press: Oxford, 1989. (b) Ziegler, T. *Chem. Rev.* **1991**, *91*, 651.

(26) Gill, P. M. W.; Johnson, B. G.; Pople, J. A. *Chem. Phys. Lett.* **1993**, *209*, 506.

(27) Johnson, B. G.; Frish, M. J. *J. Chem. Phys*. **1994**, *100*, 7429.

(28) Dirac, P. M. A. *Proc. Cambridge Philos. Soc*. **1930**, *26*, 376.

(29) Vosko, S. H.; Wilk, L.; Nsair, M. *Can. J. Phys*. **1980**, *58*, 1200.

(30) Becke, A. D. *Phys. Rev. B* **1988**, *38*, 3098.

(31) Lee, C.; Yang, W.; Parr, R. G. *Phys. Rev. B* **1988**, *37*, 785.

(32) Becke, A. D. *J. Chem. Phys*. **1993**, *98*, 5648.

(33) Pietro, W. J.; Hehre, W. J. *J. Comput. Chem.* **1983**, *4*, 241.

(34) Hay, P. J.; Wadt, W. R. *J. Chem. Phys.* **1985**, *82*, 1985.

(35) Dobbs, K.-D.; Hehre, W. J. *J. Comput. Chem.* **1987**, *8*, 880.

(36) Dunning, T. H. Jr.; Hay, P. J. In *Modern Theoretical Chemistry*; Schaefer, H. F., III, Ed.; Plenum: New York, 1976, p 1.

(37) Schwerdtfeger, P.; McFeaters, J. S.; Moore, J. J.; McPherson, D. M.; Cooney, R. P.; Bowmaker, G. A.; Dolg, M.; Andrae, D. *Langmuir* **1991**, *7*, 116.

(38) Bader, R. F. W. *Atoms in Molecules: A Quantum Theory*; Clarendon Press: Oxford, 1990.

(39) Bader, R. F. W. *Chem. Rev.* **1991**, *91*, 893.

(40) Grimme, S. *Am. Chem. Soc.* **1996**, *118*, 1529.

(41) Biegle-König, F. W.; Bader, R. F. W.; Tang, T. *J. Comput. Chem.* **1982**, *13*, 2.